

Analysis of electromagnetic and electrostatic effects of particle impacts on spacecraft

Michael C. Kelley^{a,*}, Stephanie Pancoast^{a,1}, Sigrid Close^b, Zhenzhen Wang^c

^a School of Electrical and Computer Engineering, Cornell University, 318 Rhodes Hall, Ithaca, NY 14853, USA

^b Department of Aeronautics and Astronautics, Stanford University, Palo Alto, CA 94305, USA

^c Department of Physics and Astronomy, University of Iowa, Iowa City, IA 52242, USA

Received 2 August 2011; received in revised form 23 November 2011; accepted 22 December 2011

Available online 4 January 2012

Abstract

Particle impacts on spacecraft can cause considerable damage, even leading to complete failure. A theory for the resulting vehicle potential changes and the electromagnetic radiation from impact-induced plasma has been published by Close et al. (2010). Here we compare this theory to impacts registered by the Radio and Plasma Wave Science instrumentation on the Cassini spacecraft. We study both low-velocity (16 km/s) large particles (2.6 μm radius) detected in Saturn's rings and high-velocity (450 km/s) small particles (1 nm radius) in the solar wind. The agreement with the theory is quite good. We also apply these results to earth orbit and conclude that both Electrostatic Discharge and Electromagnetic Pulse radiation are likely and could lead to spacecraft failure.

© 2011 COSPAR. Published by Elsevier Ltd. All rights reserved.

Keywords: Meteor impact; Satellite damage; High velocity impact

1. Introduction

Spacecraft are continually subject to impacts by meteoroids and space junk. The space shuttle and the International Space Station have been repeatedly hit and a space tether was severed by such an event. Such impacts can clearly have mechanical effects on spacecraft, but in recent years, evidence has arisen that electrical effects may be more important.

Two types of effects are possible (Close et al., 2010). High-velocity impacts result in vaporization/ionization of the incoming particle and spacecraft material as well. This material is thought to be ejected as energetic ions that subsequently draw out electrons (Krueger, 1996; Ratcliff et al., 1997a,b). The result is that the vehicle potential initially drops sharply, rises again as the electron emission over-

compensates positively, and then returns to its prior state by ambient plasma collection. These events may be intense enough to create an Electrostatic Discharge (ESD), which could damage spacecraft electronics.

The expanding ions can separate from the electrons by a Debye length, after which an electric field builds up to draw out the electrons. The two plasma constituents then oscillate about each other at the plasma frequency while, at the same time, the plasma expands at the ambipolar diffusion rate. This continues until electron ion collisions are sufficient to slow the expansion process to the collisional diffusion rate. As the expansion proceeds, the plasma frequency decreases, as does the frequency of the radiation generated. This electrostatic oscillation will act as an antenna and radiate electromagnetic waves, which propagate in and around the spacecraft in a phenomenon we call an Electromagnetic Pulse (EMP).

In this paper, we compare the theory proposed by Close et al. (2010) with observations of particle impacts on the Cassini spacecraft, which was instrumented with ESD and EMP detectors as well as dust/ice detectors.

* Corresponding author. Tel.: +1 607 255 7425; fax: +1 607 255 6236.

E-mail addresses: mck13@cornell.edu (M.C. Kelley), pancoast@stanford.edu (S. Pancoast), sigridc@stanford.edu (S. Close), zhenzhen-wang@uiowa.edu (Z. Wang).

¹ Now at Stanford University.

1.1. Review and analysis of ESD and EMP observations on Cassini

The Radio and Plasma Wave Science (RPWS) instrumentation on Cassini detected a high rate of impact by dusty ice particles when it penetrated the rings of Saturn (Wang et al., 2006) and the Jupiter flyby (Meyer-Vernet et al., 2009). The instrument detected pulse-like potential changes between a short monopole antenna and spacecraft ground. The ground potential pulse had the waveform,

$$V(t) = 0.4(1 - e^{-t/\tau}) \frac{Q}{C}, \quad (1)$$

where $\tau = 40$ ms, Q is the maximum charge on the spacecraft, and C is its capacitance (Wang et al., 2006). The factor 0.4 is due to a capacity divider at the amplified input. The Fourier Transform of the associated waveform is a two-component power law spectral response: f^{-2} at low frequencies (less than 4 kHz) and f^{-4} at high frequencies (4–100 kHz). This is shown here in Fig. 1. Superposed on this power law behavior was a 10 db increase in power between 40 and 80 kHz. Fig. 3 of Wang et al. (2006) shows the wavelength of a double probe detection during impact events. The initial polarity can be of either sign. This rules out vehicle potential changes since the sign of the common mode voltage would always have the same polarity. We thus conclude that the signal is due to impact on one of the probes by ejected plasma. Depending on the proximity of one or the other probes to the impact, the sign will change. Unfortunately, since we do not know where the impact occurred, we cannot interpret whether ions or electrons were ejected first.

Using Eq. (1) and a capacitance of 200 pF, the charge emissions were estimated to be 10 pC. Following work by Krueger (1996) for 15 km/s impacts of a dielectric on a metal, Wang et al. (2006) determined an rms ice particle size of 77 pg and an rms diameter of 5.2 μm for these dusty ice particles.

Dividing the emitted charge by the charge on an electron, 10 pC corresponds to 5×10^7 ions released initially,

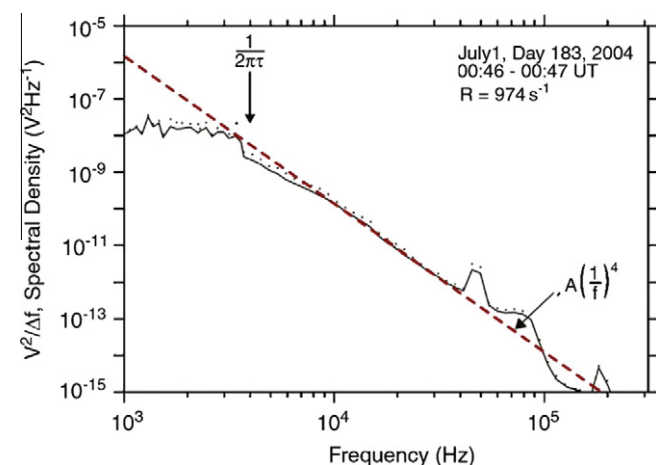


Fig. 1. Composite spectrum from many impacts. [After Wang et al. (2006). Reproduced with permission of Elsevier.]

which is followed by an equal number of ions. The expansion of the ions will occur for about one Debye length before the electrons are attracted by the ambipolar electric field. Thus, the number density at that time can be found from,

$$n = 3N/4\pi(\lambda_D)^3 \quad (2)$$

and

$$\lambda_D = (V_e)t/\omega_p, \quad (3)$$

where λ_D is the Debye length, ω_p is the plasma frequency, N is the total number of electrons emitted and $(V_e)t$ is the electron thermal speed we take to be 10^6 m/s. For a fixed T_e , Eq. (2) depends only on n and we can solve for t to find $n = 2.25 \times 10^{18} \text{ m}^{-3}$. The initial plasma frequency is thus 10 GHz. Initially, until about 10 collision times, the expansion will continue at the ambipolar rate, which is thought to be about 10^4 m/s.

We believe that the excess power in the spectrum between 40–80 kHz is oscillation of the ions and electrons at the plasma frequency, which decreases in time as the plasma expands. Only a narrow window of the plasma frequency oscillations spectrum is available due to the power spectral density in the FFT of the pulse and the upper limit of the instrument frequency response. Sixty kilohertz will be attained after about $1 \mu\text{s}$ at the ambipolar expansion rate.

The spectrum in Fig. 1 is intriguing but is a composite and cannot be used to explore the time dependence of the electromagnetic response to an impact. However, another set of impact events were recorded on Cassini (Meyer-Vernet et al., 2009) that were due to nanometer-size dust particles being accelerated by the solar wind to 450 km/s. In this case, we have the full waveform to work with, up to 110 kHz.

We have analyzed the broadband data from the dipole antenna on Cassini during such events. Because of the high common-mode rejection ratio for the system, the initial pulse caused by the vehicle potential change is greatly suppressed but the EMP is well documented. Fig. 2 shows the waveform (top panel) for one of the impacts along with a Fourier analysis (central panel) and a wavelet analysis (lower panel).

At the left-hand side of the top panel, the suppressed ESD pulse is seen as a 25 μV pulse, followed by a series of oscillations that decreases with time from about 80 kHz to less than 20 kHz during 180 ms. Fourier analysis is not well suited for analyzing such a time series, but the middle panel does show the FFT of various segments of the interval.

The wavelet analysis is much more revealing. The initial pulse is characterized by intense wavelets over the entire 32 frequency bins as befits a sharp change in the signal. This is followed by wavelet intensities that occur first at the highest frequency and then progress to the lower frequencies over time. For reference, the unity scale wavelet has a characteristic time of 0.67 ms.

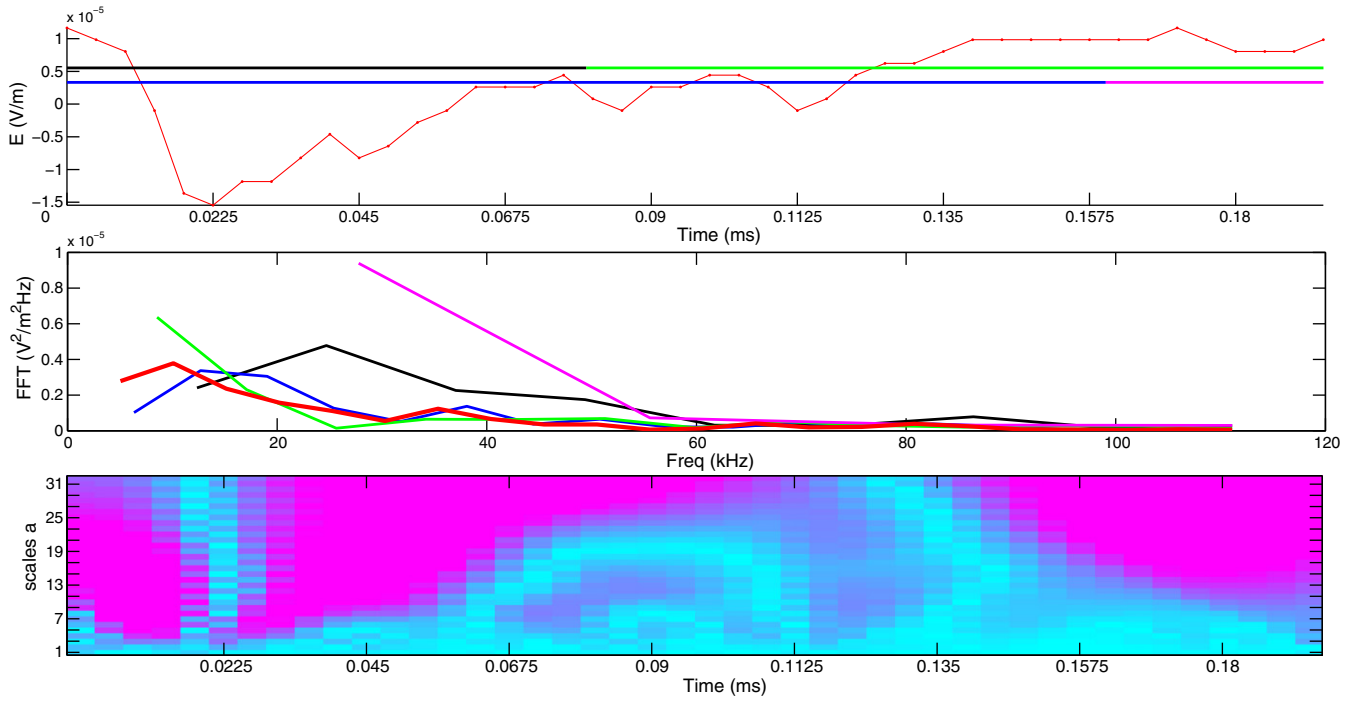


Fig. 2. Waveform, Fourier analysis, and wavelet analysis for the impact of nanometer-size particles at solar wind velocity on Cassini. A symlet order-2 wavelet was used. The scale $a = 1$ corresponds to the frequency >148 kHz and scale $= 32$ corresponds to 4.7 kHz.

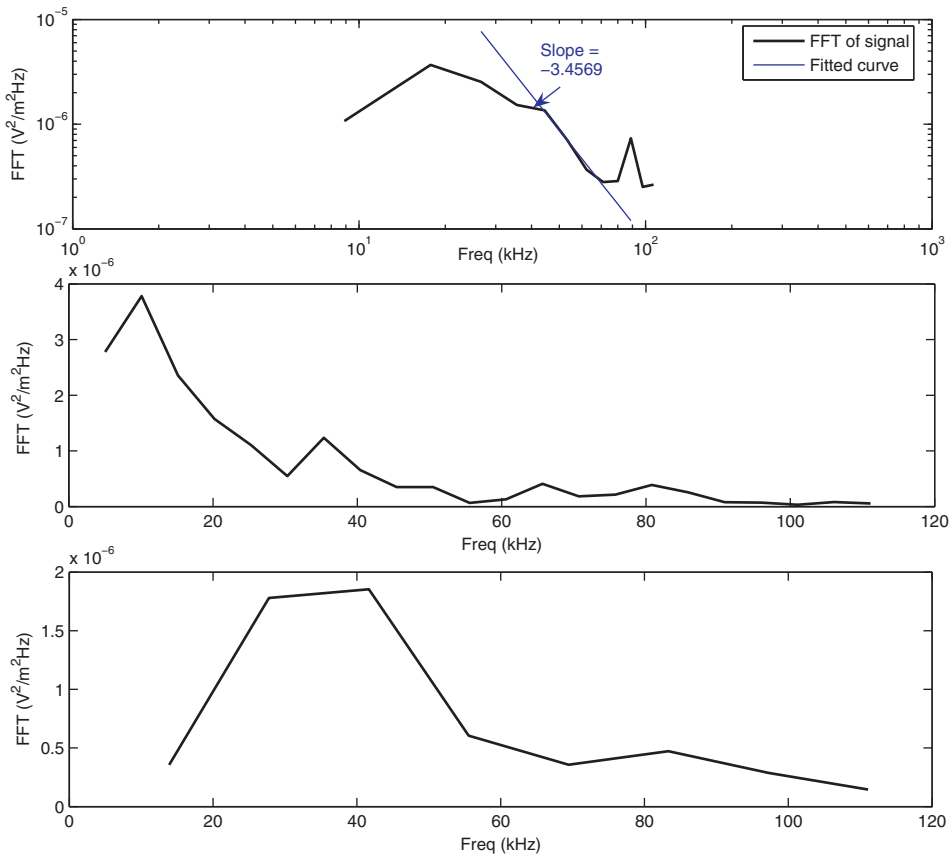


Fig. 3. Three spectral presentations. The top panel is a log-log plot of the first third of the data set. The middle panel covers the whole period in a log-linear format. The lower panel does not include the pulse.

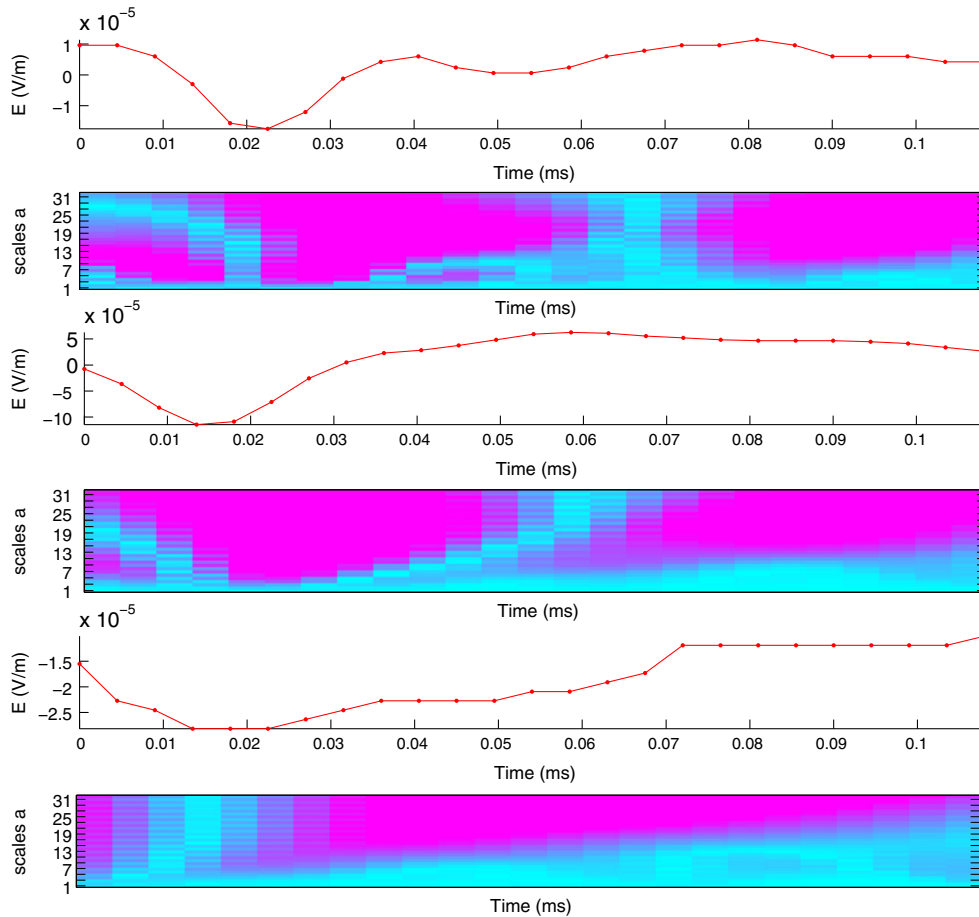


Fig. 4. Three more examples of waveforms and wavelet analysis for dust impacts. The scales are identical to those in Fig. 2.

In Fig. 3 we replot the various spectra using log–log and log–linear axes. The top panel is for the first third of the period, which includes the pulse. We see an f^{-2} power law followed by an f^{-4} power law, as is also found in Fig. 1. The middle panel is the FFT of the whole interval, whereas the lower panel begins at 10 ms and does not include the pulse. Evidence for high-frequency oscillations is seen when the pulse is absent or when the frequency is high enough for the power to exceed that of the pulse spectrum.

In Fig. 4 we present three more examples of waveforms and wavelet analysis for dust impacts. In each case, the pulse and oscillations are seen.

To study this quantitatively, we follow Meyer-Vernet et al. (2009) and Close et al. (2010) for nanoparticles at these high velocities. The former authors calculate that the charge release was 5×10^{-13} C. Dividing by the charge on an electron yields 3×10^6 particles. Note that the plasma expands for 0.225 ms before we first can measure the plasma frequency since, before this, the vehicle potential change dominates the signal. Ratcliff et al. (1997a,b) predict an expansion velocity of 10 km/s, which yields a diameter of 2.25 m at that time and a plasma density of $84,000 \text{ m}^{-3}$ for a sphere and twice that for a half sphere. The plasma frequency at that time is thus 2600–3600 Hz, in reasonable agreement with the data. Since the volume

increases as t^3 , the plasma frequency at 10 times the delay should be 260–360 Hz, which is also in good agreement with the data.

2. Scaling to other impacts

Close et al. (2010) and Stewart and Valiant (2006) studied the impact effects over a wide range of metallic (meteoroid) impact particles. To scale this to earth-orbiting satellites impacted by meteors, we need to increase the differential velocity to as high as 45 km/s, which increases the Q release to 1000 C/g (Lee et al., 2012). Since the vehicle potential changes scales with this differential Q , we find that it rises from the 20 mV measured on Cassini to 500 V (for metallic impactors of the same size as those in the Cassini case). The released charge scales linearly with mass and as $V^{3.8}$ (Lee et al., 2012), so very large potentials are possible. There is thus a definite possibility that an Electrostatic Discharge (ESD) is possible for impacts on the spacecraft ground plane. Note that the Cassini impacts are thought to have been on the large conducting high-gain antenna.

Hoerz et al. (1975) and Stewart and Valiant (2006) developed a crater impact theory and compared it favorably with data for Martian craters. If we extrapolate these data to the rms particle size detected on Cassini, a diameter

of $5.2 \mu\text{m}$, the ejected volume is 10^{-8} m^{-3} , corresponding to a linear dimension of 0.22 cm . For impact of aluminum on aluminum, this corresponds to 6.3×10^{20} atoms. For an impact of ice on aluminum, we lower this by a factor of 10. Finally, since the impact velocity on Mars is about 1.7 times higher than ice on Cassini and the particle release varies as the velocity to the fourth power, we lower this by another factor of $30\text{--}2.1 \times 10^{19}$. Dividing by the initial volume found above yields a neutral number density of $3 \times 10^{22} \text{ m}^{-3}$. The number density of plasma particles was found above to be $n = 2.25 \times 10^{18}$. The low ratio of charged particles to neutral atoms available strongly suggests that most of the charge is tied up on dust particles. Murr and Rivas (1994) studied the re-coagulation of atoms from ablating meteors. They found that for meteors larger than 10 g, re-coagulation proceeds exponentially. Of course, the number density of the tail for such a large meteoroid would be much smaller than an impact event of the same size, so re-coagulation is very fast.

We turn now to the case of 6 nm particles traveling at solar wind speeds (450 km/s). The comparison with Martian craters does not work as well for such small particles and we work the problem backwards. At .27 ms, the expanding sphere is 2.7 m in diameter and the oscillation frequency is 5 kHz. This corresponds to a plasma density of $3.1 \times 10^5 \text{ m}^{-3}$ and a total number of ejected ions of 2.4×10^7 . A 6 nm particle would make a crater about 10 times its diameter at 40 km/s. For a hemisphere, the volume would be $4.3 \times 10^{-22} \text{ m}^{-3}$. The volume scales as V^2 so, at 400 km/s, it would be $4.3 \times 10^{-20} \text{ m}^{-3}$. Aluminum would hold 5×10^4 particles. Since the incoming particle is the same size, this estimate yields 4×10^6 particles, a factor only five times lower than the data suggest. The vehicle potential is not likely to be affected by these particles.

3. Summary and conclusions

We have compared observations of high-velocity impacts on the Cassini spacecraft with the theory of Close et al. (2010). We find excellent agreement with both the vehicle potential changes and the plasma oscillations for large, low-velocity particle impacts and for small, hyper-velocity particles.

When applied to particle impacts on earth-orbiting satellites, our first conclusion is that very high vehicle poten-

tial changes are possible for hyper-velocity metallic impacts on spacecraft ground, which could lead to ESD failures. We also find that an Electromagnetic Pulse will be generated and radiated by such impacts.

Acknowledgements

This research at Cornell University was supported in part by the Office of Naval Research under grants N00014-09-1-1130 and N00014-09-1-0975 and by the NASA/New York Space Grant Consortium. Work at Stanford University was supported by a contract through Los Alamos National Laboratory.

References

- Close, S., Colestock, P., Cox, L., Kelley, M., Lee, N. Electromagnetic pulses generated by meteoroid impacts on spacecraft. *J. Geophys. Res.* 115, A12328, doi:10.1029/2010JA015921, 2010.
- Hoerz, F., Morrison, D.A., Brownlee, D.E., Fechtig, H., Hartung, J.B., Neukum, G., Schneider, E., Vedder, J.F., Gault, D.E. Lunar micro craters – Implications for the micrometeoroid complex. *Planet. Space Sci.* 23, 151–172, 1975.
- Krueger, F.R. Ion formation by high- and medium-velocities dust impacts from laboratory measurements and Halley results. *Adv. Space Res.* 17 (12), 71–75, 1996.
- Lee, N., Close, S., Lauben, D., Linscott, I., Goel, A., Johnson, T., Yee, J., Fletcher, A., Srama, R., Bugiel, S., Mockler, A., Colestock, P., Green, S. Measurements of freely-expanding plasma from hypervelocity impacts. *Int. J. Impact Eng.*, in press, 2012.
- Meyer-Vernet, N., Lecacheux, A., Kaiser, M.L., Gurnett, D.A. Detecting nanoparticles at radio frequencies: Jovian dust stream impacts on Cassini/RPWS. *Geophys. Res. Lett.* 36 (3), L03103, doi:10.1029/2008GL036752, 2009.
- Murr, L.E., Rivas, J.M. Measuring hypervelocity impact velocity from micrometeoroid crater geometry. *Int. J. Impact Eng.* 15 (6), 785–795, 1994.
- Ratcliff, P.R., Burchell, M.J., Cole, M.J., Murphy, T.W., Allahdadi, F. Experimental measurements of hypervelocity impact plasma yield and energetics. *Int. J. Impact Eng.* 20 (6-10), 663–674, 1997a.
- Ratcliff, P.R., Reber, M., Cole, M.J., Murphy, T.W., Tsembelis, K. Velocity thresholds for impact plasma production. *Adv. Space Res.* 20 (8), 1471–1476, 1997b.
- Stewart, S.T., Valiant, G.J. Martian subsurface properties and crater formation processes inferred from fresh impact crater geometries. *Meteoritics Planet. Sci.* 41 (10), 1509–1537, 2006.
- Wang, Z., Gurnett, D.A., Averkamp, T.F., Persoon, A.M., Kurth, W.S. Characteristics of dust particles detected near Saturn’s ring plane with the Cassini Radio and Plasma Wave instrument. *Planet. Space Sci.* 54 (9–10), 957–966, 2006.